Computer Aided Geometric Design ••• (••••) •••–•••

Contents lists available at ScienceDirect

Computer Aided Geometric Design

www.elsevier.com/locate/cagd

Medial axis tree—an internal supporting structure for 3D printing

Xiaolong Zhang [a,*], Yang Xia [a,b,*], Jiaye Wang [c], Zhouwang Yang [d], Changhe Tu [c], Wenping Wang [a]

[a] The University of Hong Kong, Hong Kong
[b] Dalian University of Technology, China
[c] Shandong University, China
[d] University of Science and Technology of China, China

ARTICLE INFO

Article history:
Received 21 February 2015
Accepted 11 March 2015
Available online xxxx

Keywords:
Supporting structure
3D printing
Medial axis transform

ABSTRACT

Saving material and improving strength are two important but conflicting requirements in 3D printing. We propose a novel method for designing the internal supporting frame structures of 3D objects based on their medial axis such that the objects are fabricated with minimal amount of material but can still withstand specified external load. Our method is inspired by the observation that the medial axis, being the skeleton of an object, serves as a natural backbone structure of the object to improve its resistance to external loads. A hexagon-dominant framework beneath the boundary surface is constructed and a set of tree-like branching bars are designed to connect this framework to the medial axis. The internal supporting structure is further optimized to minimize the material cost subject to strength constraints. Models fabricated with our method are intended to withstand external loads from various directions, other than just from a particular direction as considered in some other existing methods. Experimental results show that our method is capable of processing various kinds of input models and producing stronger and lighter 3D printed objects than those produced with other existing methods.

1. Introduction

Fabricating various objects with 3D printing is getting increasingly popular with the availability of affordable FDM 3D printers. Saving both material and printing time while not compromising structural strength or altering the appearance of the model, is a major consideration for 3D printing users. Therefore, it is important to design a strong and light-weight model while not affecting the original shape and feel of an object. This entails the design of internal supporting structures for 3D printed objects.

Our key observation is that the medial axis can serve as the basis for an internal structure designed to enhance the strength of the printed model. From a biomimetic viewpoint, the medial axis is analogous to the skeletal structure, which has similar topological and geometric structure, as shown in Fig. 1. Therefore, the medial axis can function as a skeleton system, dispersing and absorbing the loads applied to the object while remaining stable. Mechanically, the medial axis is at the central location to place supporting material, which is also an observation made by researchers in topological

* Corresponding authors at: The University of Hong Kong, Hong Kong.
E-mail addresses: xlzhang@cs.hku.hk (X. Zhang), xiayangdlut@gmail.com (Y. Xia).

http://dx.doi.org/10.1016/j.cagd.2015.03.012
0167-8396/

Please cite this article in press as: Zhang, X., et al. Medial axis tree—an internal supporting structure for 3D printing. Comput. Aided Geom. Des. (2015), http://dx.doi.org/10.1016/j.cagd.2015.03.012

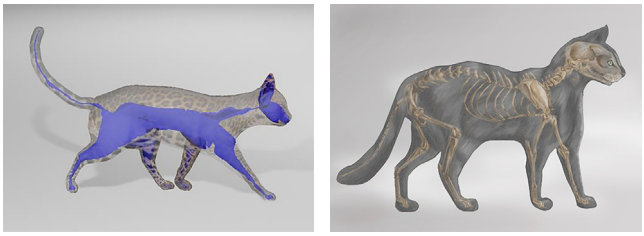

(a) Medial Axis (b) Skeletal Structure

Fig. 1. The medial axis and skeletal structure of a kitten respectively, showing the analogy between them.

optimization (Bremicker et al., 1991). 3D printed objects are usually handled by human with pinch force, where the symmetry property of medial axis could help cancel loads like this, which makes the medial axis a good candidate to serve as a supporting structure core.

For an animal-shaped object, the medial axis is not identical to the biological skeletal structure. However, we argue that the medial axis is more suitable than the skeletal structure for 3D printing. First, the skeletal system has biological functions of protecting viscera, which is not required of 3D printed object; in contrast, the medial axis can make full use of the internal space. Furthermore, the medial axis can provide support for small features of the printed model, such as the ears in Fig. 1, which cannot be fulfilled by skeletal.

We shall propose a new kind of internal supporting structure, called the *medial axis tree*, and present a method for computing it for cost-effective 3D printing of strong and light-weight objects. For an input 3D object to be printed, this supporting structure is composed of three components: (1) the *medial structure*, which is a central supporting structure lying near the medial axis of the input object; (2) the *boundary framework*, which is a hexagonal framework beneath the boundary surface of the object; and (3) the group of *connecting bars* which connects the boundary framework with the medial structure to form the complete internal supporting structure.

In our design, the medial structure serves as the foundation of the whole supporting structure, the group of tree-like connecting bars serves as intermediate elements to support the boundary framework beneath the boundary surface, and the boundary framework helps to disperse external loads and to resist shape deformation by passing external forces through the connecting bars to the medial structure. These three components work together as an integrated supporting system.

The medial axis tree designed with our algorithm can maintain the required strength of printed objects with a minimal amount printing material, consequently saving the cost and the printing time. We validated our method by printing a large number of models and carried out both numerical simulations and physical experiments.

The following contributions are made in this work:

- We propose a new type of internal supporting structure for 3D printing, called *medial axis tree*, based on the medial axis. The medial axis provides a sound foundation for the structure to resist external loads from various directions and the tree structure helps transmit loads from the boundary surface to the medial axis.
- We propose to use a hexagon-dominant framework as the supporting structure beneath the surface of objects. This surface framework possess high strength to weight ratio, and exhibit excellent energy absorption properties.
- We present an effective optimization scheme for improving the design of the internal supporting structure, by considering combined load conditions. To improve computational efficiency, we propose a partition-based structure optimization method to greatly reduce the number of design variables.

2. Related work

2.1. Structure design for 3D printing

Stava et al. introduced various methods in (Stava et al., 2012) for enhancing the strength of a printed object by detecting structural problems and correcting them by hollowing, thickening and truss insertion so that the printed model can be modified to be structurally sound. However, they only focus on enhancing the structure stability while not taking material cost into consideration.

Various works focus on the efficient methods for distributing material within model's body. The hollowing method is used by most commercial printing software packages (Shapeways, 2012). It is easy to implement by extruding the outer surface inwards, but it is difficult for users to determine a proper thickness of the boundary shell. Wang et al. (2013) reduced model's material cost while retaining its mechanical structure strength by presenting a skin-frame structure similar to the truss structure used in structural engineering. In their method, a set of points are distributed on the surface and within the body of the objects, and an initial frame structure randomly connecting these points is created. Then the size, topology and geometry of the frame structure are optimized to improve the initial structure to a more cost-effective one.

There are several aspects of the method by Wang et al. (2013) that call for improvement. First, because of the complexity in structure optimization, the optimization speed is slow and not guaranteed to yield a global optimal solution. Second, the

Please cite this article in press as: Zhang, X., et al. Medial axis tree—an internal supporting structure for 3D printing. Comput. Aided Geom. Des. (2015), http://dx.doi.org/10.1016/j.cagd.2015.03.012

initial random structure may not be an ideal initial configuration to start with for the optimization. Third, the resulting structure highly depends on the direction of the given force load, which means that the obtained structure may not be effective for the loads from other directions. In comparison, the supporting structure we proposed takes the advantage of the medial axis, a structure that naturally transfer the external loads from different directions to the inner core structure. This significantly increases the model stability even with different loading conditions.

Recently Lu et al. (2014) presented a honeycomb-cell structure by gradually carving out the interior of an object to be printed. They present an aesthetic design for inner structure, but the hollowed cells within the solid are not connected. That makes it difficult to remove the soluble supporting materials in the case of using stereolithography method for 3D printing or power-based 3D printing.

2.2. Medial axis transform

The medial axis of an object was first proposed by Blum et al. (1967) for biological shape measurement. It is a skeletal representation defined as the set of the centers of inscribed spheres touching the object boundary in at least two points (Culver et al., 1999). The medial axis is used in applications ranging from feature recognition, finite element mesh generation to path planning. Many methods have been proposed for efficient medial axis computation (Foskey et al., 2003), such as the λ-medial axis (Chazal and Lieutier, 2005; Chaussard et al., 2009), and the Scale Axis Transform (SAT) (Giesen et al., 2009; Miklos et al., 2010). As the basis for our medial structure computation we use the SAT method to generate a simplified medial axis. SAT removes the inherent sensitivity of the medial axis and provides an efficient and simple way of generating a simplified medial axis.

2.3. Hexagon surface structure

Nieser et al. (2012) introduced a method of generating regular hexagons for arbitrary surfaces with the sides of the hexagons aligned with the underlying surface features. Pietroni et al. introduced Voronoi grid-shell structures with Anisotropic Centroidal Voronoi Tessellation and the resulting mesh was hex-dominant. It was further demonstrated that the obtained hex-dominant mesh achieve better static performance, compared with quad-based grids (Pietroni et al., 2014). Jiang et al. (2014) designed the free form honeycomb structure for torsion-free structures.

3. Problem and algorithm overview

3.1. Problem

Given a model for printing, our goal is to create an internal supporting structure based on the model's medial axis, in order to ensure sufficient strength for the model to withstand expected external loads for its intended function or handling. We assume that the design of the input model is structurally sound, since existing software programs are capable of identifying and correcting structural defects (Meshmixer, 2014). Hence, we do not make any change to the appearance of the input model.

The supporting structure we proposed is called *medial axis tree*, shown in Fig. 2. It consists of three components: (1) the *medial structure*; (2) the *boundary framework*; and (3) the group of *connecting bars* connecting the medial structure and the boundary framework. Optimization and mechanical analysis considering various typical force loading conditions are carried out to produce the optimized structure. The boundary surface is printed outside this supporting structure to maintain the original appearance of the input object.

3.2. Algorithm overview

In this section we shall briefly introduce the pipeline of our proposed method. It consists of two steps: (1) designing the initial *medial axis tree*; and (2) optimizing the *medial axis tree* by taking into consideration of various typical external load conditions.

3.2.1. Medial axis tree

The medial axis tree structure is composed of three components, as shown in Fig. 2. Given a boundary representation of a 3D object (Fig. 3(a)), we first compute its medial axis using the scale axis transform (Giesen et al., 2009) which is shown in Fig. 3(b). Then we compute the Restricted Centroid Voronoi Tessellation (RCVT, shown in Fig. 3(c)) using method described in (Yan et al., 2009), to get a hexagonal frame structure (Fig. 3(d)). We call it a hexagonal frame because most of the polygonal cell are hexagons, with a few exceptional pentagons to accommodate for the surface topology and curvature variation. We then take all the vertices of the hexagonal frame (Fig. 3(e)) and project it to its corresponding points on the medial axis (Fig. 3(f)). The projection is done by finding its medial axis ball center for each point in Fig. 3(e). These corresponding points are connected, as shown in Fig. 3(i).

To make forces from the opposite directions balance each other, we group the nearby points on the medial axis (Fig. 3(g)) and obtain clustered medial axis trees (Fig. 3(j)). Also, the other problem is the unacceptable slenderness ratio (length over

Please cite this article in press as: Zhang, X., et al. Medial axis tree—an internal supporting structure for 3D printing. Comput. Aided Geom. Des. (2015), http://dx.doi.org/10.1016/j.cagd.2015.03.012

Nomenclature

E	Young's modulus	$\sigma_{\max}$	Yield stress
v	Poisson's ratio	η	Printer's precision
I	Inertia moment	h	Surface's thickness
D	Bending strength	r	Strut's radius

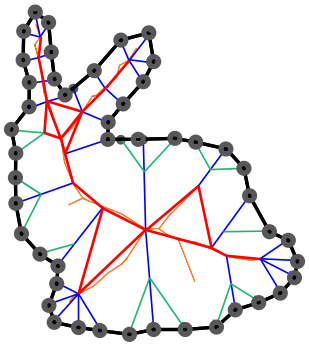

Fig. 2. Illustration of the medial axis tree structure for a 2D shape. It is composed of three parts: the hexagon surface grid in black, the tree-like supporter in blue and green (green bars indicates tree-like connecting structures), and the tree root connector in red. The medial axis of the original shape is shown in orange. These three parts have different structural functions and are combined to form an internal supporting structure. (For interpretation of the references to color in this figure legend, the reader is referred to the web version of this article.)

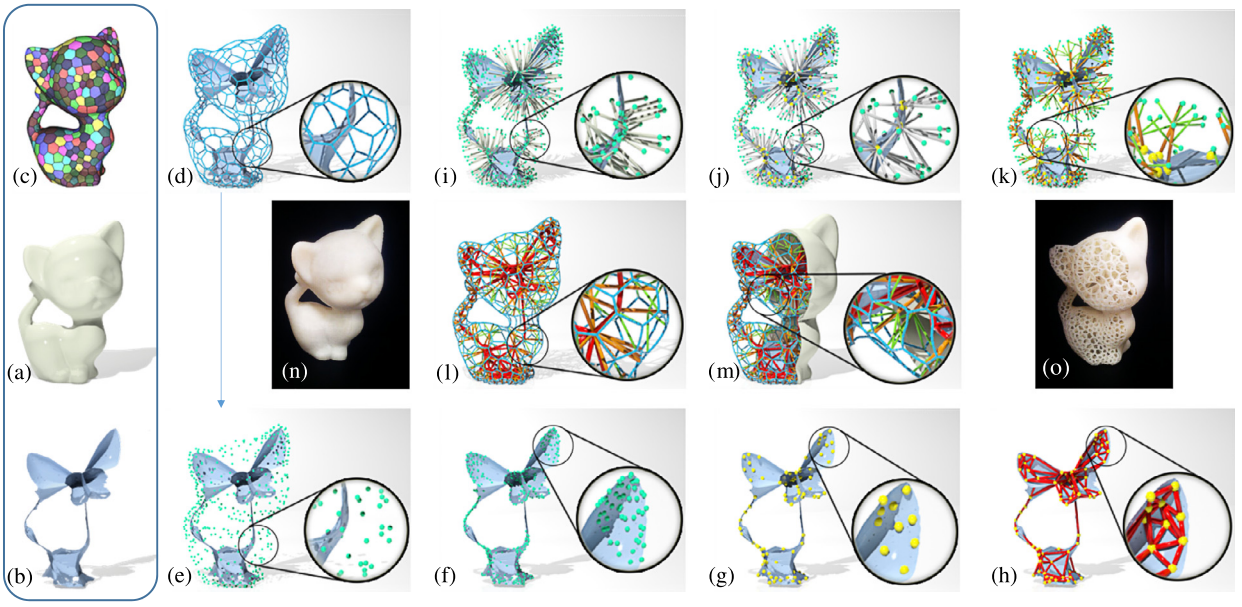

Fig. 3. The workflow of computing the Medial Axis tree. (a) the input mesh; (b) the medial axis; (c) and (d) the RCVT remesh and the hexagon frame structure; (e) the sampling points on surface; (f) the projection of the sampling points in MA; (g) the point clustering; (h) the tree root connector; (i) initial connecting bars; (j) connecting bars after clustering; (k) adaptive tree-like connecting bars; (l) and (m) a view of the Medial Axis Tree structure; (n) and (o) shows the printed result of kitten model and our supporting structure.

radius) if the model has sub-parts similar to spheres. Struts with high slenderness ratio will bend under pressure thus cannot transfer the external loads to the medial axis anymore (Fig. 4).

Instead of increasing radii to all the struts, we do clustering again on the hexagon surface vertices with high slenderness ratio and select struts connecting the cluster center as main struts whose radii are increased, and lift other struts along these main struts to reduce their length (thus avoiding high slenderness ratio). This process is shown in Fig. 3(k).

We use a frame structure to approximate the input object's medial axis, which is in general a 2D surface. The resulting frame structure is shown in Fig. 3(h). Finally, all the three components of our supporting structure are combined and shown

Please cite this article in press as: Zhang, X., et al. Medial axis tree—an internal supporting structure for 3D printing. Comput. Aided Geom. Des. (2015), http://dx.doi.org/10.1016/j.cagd.2015.03.012

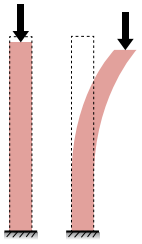

Fig. 4. Buckling of struts with high slenderness ratio under pressure.

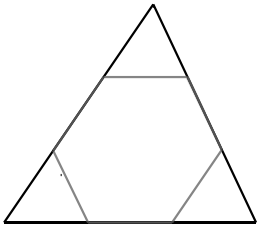

Fig. 5. Inscribed hexagon of a triangle.

in Fig. 3(l) and (m). Fig. 3(n) shows the printed model and the corresponding medial axis tree structure can be seen in Fig. 3(o).

3.2.2. Pipeline of optimization

The medial axis tree structure created by the pipeline described above provides a reasonable initial structure. We further improve this structure by optimizing the topology and volume of the structure to reduce the usage of printing material subject to the strength and deformation constraints. The struts in the structure are classified into groups, where struts in the same group share the same radius so that the total number of optimization variables is significantly reduced, thus the optimization time is reduced as well.

The result of the optimization process is largely affected by the prescribed force load. In this work we consider the combination of various external load conditions, which is the concept of "load combination" in civil engineering (Wen, 1990). Note that this is different from some other methods (Wang et al., 2013; Lu et al., 2014) that consider only a specific load with a particular direction. There are two steps to determine the combined load condition in optimization. First, the locations and directions of loads corresponding to main working conditions are recognized by analysis of the model's convex hull. Then the magnitude of each load are determined by considering the probability of the corresponding working condition. The combination of the loads are applied in the optimization process. The whole process of optimization is concluded as in Algorithm 1:

Algorithm 1 Optimization process.

Require: Medial axis tree (MA Tree) structure.
Ensure: Optimized MA Tree structure.
Step 1: Convex hull analysis and load combination.
Step 2: Mechanical analysis and radii classification.
Step 3: Topology and volume optimization.

4. Algorithm details

4.1. Hexagon surface frame generation

We choose hexagon surface frame to represent the surface mesh because it has favorable mechanical and geometric property. Hexagon structures possess high strength to weight ratio, and exhibit excellent energy absorption properties (Ali et al., 2008). They are used in various engineering situations like railway, automobile and aircraft, to improve the strength-to-weight ratio or to absorb energy in accidental impacts. In natural world the honeycomb is an ingenious hexagonal structure, which is lightweight and durable. Recently Lu et al. proposed a honeycomb structure to create cost effective design for 3D printing (Lu et al., 2014). Hexagon framework also has improved aesthetic properties, as shown in work by Pietroni et al. (2014).

Compared with triangle mesh, hexagon mesh enjoys better mechanical properties with same volume of material, which can be proved from the following observation. For a given triangular mesh, a hexagon mesh with fewer quadrilaterals, pentagons or triangles can be created that both the total length of edges and the area covered of the meshes are same, and the hexagon mesh has denser, shorter edges and better geometry property. An illustration is given in Fig. 5, showing that for each triangle, an inscribed hexagon which has same ratio of total length to area with triangle can be created, and the edge's length in the hexagon is only one third of that in triangle.

We compute the Restricted Centroid Voronoi Tessellation using method described in (Yan et al., 2009), to get a hexagonal frame structure. As RCVT produces a hexagonal structure restricted to the input boundary surface mesh, this structure matches the exact shape of the input model and therefore reserves most of its geometric features.

Please cite this article in press as: Zhang, X., et al. Medial axis tree—an internal supporting structure for 3D printing. Comput. Aided Geom. Des. (2015), http://dx.doi.org/10.1016/j.cagd.2015.03.012

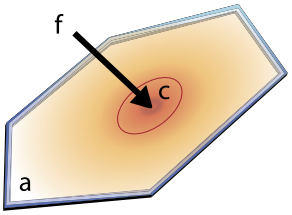

Fig. 6. Physical model illustration for local deformation control on surface. A circular plate under uniformly distributed load is used to approximate the hexagon plate problem. The boundary of the plate is fixed.

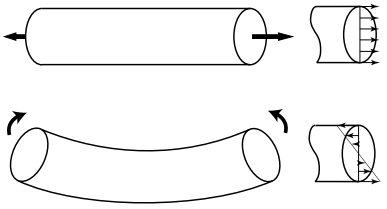

Fig. 7. Normal stress distribution on the section of beam under stretch and bending. The torsion deformation does not create normal stress.

4.2. Local deformation control

To save material, we intend to use a sparse surface framework, since the number of the mesh vertices determines the number of struts used to connect to the medial structure. As mentioned in Section 1, the function of the surface frame structure is to help resist the deformation of surface skin and to transfer the external loads to the medial structure. According to this design, suppose we apply a uniformly distributed force, denoted as f, which is perpendicular to the surface (Fig. 6) and the area under load forms a circle with radius c. Let a be the edge length of a typical hexagon of the underlying grid. The boundary of surface is assumed to be firmly supported by the hexagonal grid and the displacements on the boundary vanishes. According to the elastic plate theory introduced by Timoshenko's classic work (Timoshenko et al., 1959), the maximum deformation of a circle plate with radius a under distributed load q applied on the ring with radius b and width db, which in total is $f_c = q \cdot 2\pi b \cdot \mathrm{d}b$, can be calculated, as shown in Eq. (1), where D is the bending strength. It follows that, with the superposition method by setting the load on the ring as infinitesimal, we derive the formula for calculating the maximum deformation $w_{\max}$ by integrating on the circle domain according to variable b and then multiplying the obtained formula with correction factor k. So the maximum deformation of a typical hexagon patch under load can be calculated as shown in Eq. (3). The correction factor k is set to be 0.8 by the standard numerical analysis using the finite element method. This formula has been validated to yield accurate prediction.

$$w_{cirlce} = \frac{f_c}{8\pi D}\left[b^2 \ln\left(\frac{b}{a}\right) + \frac{a^2 - b^2}{2}\right] \tag{1}$$

$$D = \frac{Eh^3}{12(1-v^2)} \tag{2}$$

The maximum deformation $w_{\max}$ is expected to be less than some upper bound of deformation, denoted by $\bar{w}$. With this constraint, the upper bound of a, denoted as $\bar{a}$, is determined as well, and the minimum sampling number is obtained as $\frac{S}{1.5\sqrt{3}\bar{a}^2}$, where S is the surface area of the given model. Considering that non-uniform hexagon mesh is used and the length of bars varies, the sampling number should be larger than the minimum number. For ABS printing material, the Young's modulus is $E = 1807$ MPa (Mega Pascals) (Tymrak et al., 2014) and the Poisson's ratio is $v = 0.35$. We set $f = 0.5$ N, which is approximately the weight of an egg, $c = 5$ mm, $h = 0.254$ mm, which is the same as the precision of uPrint SE Plus printer, and $\bar{w} = 1$ mm in our implementation. The corresponding upper bound of edge length is $\bar{a} = 0.02$ m. Formula (3) can also give suggestion on the thickness h of outer surface, and helps to control the local deformation of outer boundary surface.

$$w_{\max} = k\int_0^c w_{circle} = k\frac{f}{16\pi D}\left[c^2 \ln\frac{c}{a} + a^2 - \frac{3}{4}c^2\right] \tag{3}$$

The radius of the bars are also bounded with a deformation limit. Suppose that a bar in the hexagon is bounded at both ends and a load in the middle of the bar is applied. The largest deformation is calculated using Eq. (4), which should also be less than $\bar{w} = 1$ mm, $w_b < \bar{w}$. The lower bound of the radius can be calculated using Eq. (5). Set $P = f/6 = 0.5/6$ N, $l = \bar{a} = 0.02$ m, $\bar{w} = 0.001$ m, $I = \pi r^4/4$, then we can get $r > 0.2224$ mm.

$$w_b = \frac{1}{192}\frac{Pl^3}{EI} \tag{4}$$

$$r > \sqrt[4]{\frac{Pl^3}{48\pi E\bar{w}}} \tag{5}$$

Please cite this article in press as: Zhang, X., et al. Medial axis tree—an internal supporting structure for 3D printing. Comput. Aided Geom. Des. (2015), http://dx.doi.org/10.1016/j.cagd.2015.03.012

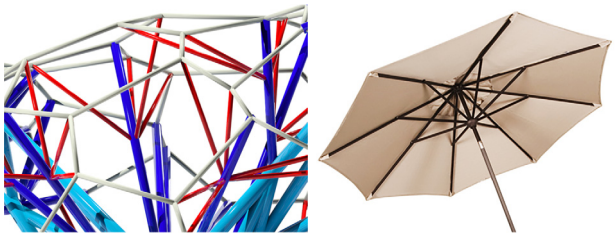

(a) Tree-like structure (b) An umbrella

Fig. 8. Tree like supporting structure obtained by our algorithm has similar structure and design with a umbrella.

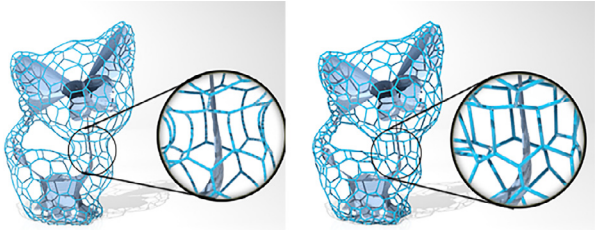

(a) Curved hexagon mesh (b) Straight hexagon mesh

Fig. 9. The difference in geometry introduced by replacing the curved hexagon mesh with straight one is insignificant and does not affect the precision of simulation results.

4.3. Adaptive branching trees

For supporting the hexagonal surface structure, a strut, which lies roughly along the surface normal direction is used to connect each of its vertices to a corresponding vertex of the medial axis surface, as shown in Fig. 3(i). In order to use only a moderate number of such connecting struts, we need to cluster the vertices of both the boundary frame structure and the medial axis structure to produce simplified meshes for these two structures with a reduced number of vertices.

4.3.1. Clustering on the medial axis

The most common external loads of an object are pinch by human handlers, with the typical configuration of fingers pressing the opposite sides of the object. Our observation is that if the struts supporting two pinch points have a common base on the medial structure, then pinch loads can be balanced in a stable manner. To facilitate this design, we use K-medoid clustering (Park and Jun, 2008) to merge the vertices to produce a simplified medial structure. K-medoid clustering is a variant of traditional K-means clustering with the constraint that each cluster center must be at the location of one of the original mesh vertices, ensuring that the simplified medial structure well approximates the original medial structure. The cluster number k is a user defined value and is set to be $n/5$ in our implementation, where n is the number of the mesh vertices before simplification. We use geodesic distance between two points on the medial axis as the distance metric for clustering.

4.3.2. Tree-like connecting structures

Connecting bars are used to connect the boundary frame and the medial structure. The most straightforward design of the connecting bars are individual straight, cylindrical struts. However, a difficulty arises if these bars have to be very long in the case of large radius in the medial axis transform, which occurs, for example, for sphere-shaped object. On one hand, the radius of these struts would have to be large as well to avoid thin and long bars which yield easily under external loads. On the other hand, simply increasing the radii of the struts would result in excessive use of printing materials.

We resolve this difficulty by introducing in this case a tree-like connecting structure to replace a cylindrical strut. A tree-like structure has a thick trunk that stems from the medial axis and branches into a number of relatively thin rods to reach the boundary surface frame, which has a similar structure like umbrella, as shown in Fig. 8. Consequently, only relatively small number of tree structures are needed and sufficiently many rods at the top of the trees are provided to support the boundary framework. In this way, the total printing material is saved, compared with simply making all the bars thicker.

We use again K-medoid clustering for selecting the main struts (or trunks) for designing the tree-like connecting structures. By clustering only on hexagon surface vertices whose connecting bars have large slenderness ratio, we select the struts connecting the resulting clustering centers as main struts. The cluster number k is a user defined value and our empirical value is $n/4$ where n is the total number of points to cluster. We use geodesic distance on the hexagonal mesh surface as metric between two points. We define the branching point at the 2/3 of the length of a tree-like connecting

Please cite this article in press as: Zhang, X., et al. Medial axis tree—an internal supporting structure for 3D printing. Comput. Aided Geom. Des. (2015), http://dx.doi.org/10.1016/j.cagd.2015.03.012

structure from its "root". Note that this operation of introducing tree-like connecting structures is only performed for long slender struts, since there is no need of it for short struts.

4.4. Constructing medial supporting structure

In the following we describe how to compute the medial supporting structure. The medial axis of an input object is first approximated by a dense triangle mesh computed using the SAT method (Giesen et al., 2009; Miklos et al., 2010). Then this initial dense mesh is simplified using a vertex-merging approach to produce a triangle mesh of appropriate vertex density. The medial supporting structure is derived from this simplified mesh and a strong framework is obtained to support the boundary surface framework.

5. Mechanical analysis and optimization

5.1. Mechanical analysis

The medial axis tree structure we propose is essentially a frame structure composed of cylindrical struts. A simplification is made that the mesh of hexagon surface structure, in which each side of hexagon created by RCVT is composed of a few connected short bars, is simulated by a mesh with straight struts. The difference in geometry introduced by this simplification is insignificant and does not affect the precision of simulation results, but greatly improves the efficiency in analysis (see Fig. 9). We use the finite element method for mechanical analysis and the 3D beam elements to simulate the property of supporting structures. The effect of the three kinds of deformations, i.e. the axial compression or tension, torsion and bending are considered. The general stiffness equation is given by the finite element formulation, which is given in detail in (Chandrupatla et al., 1991).

5.1.1. Stress analysis

Typical stress states for beam are combined effect of the three deformation types. Note that the stress distribution on the beam section generated by different deformation shapes are different, as shown in Fig. 7. In our formulation, the largest normal stress on the outer edge of the section is chosen as the critical stress. We compute the stress σ on each strut, using Eq. (6), in which M stands for the absolute value of bending moment, I the inertia moment, F the absolute value of axial force, A the area, and r the radius.

$$\sigma = \frac{Mr}{I} + \frac{F}{A} \tag{6}$$

5.1.2. Mechanical constraints

When designing a supporting structure, we need to consider various constraints in order to make the structure mechanically stable and printable.

1. *Mechanical strength*: The mechanics of frame structure has been studied based on beam theory (Hughes, 2012) where struts are assumed to behave like simple beams under linear deformation. To keep the structure durable under the specified force, we add a constraint of stress on each strut $\mathbf{e}_j$ which satisfies

$$\sigma_i \leq \sigma_{\max} \tag{7}$$

where $\sigma_{\max}$ is the maximum tolerable yield stress of the printing material (e.g., 41 MPa for ABS material), and σ_i is the stress σ in $\mathbf{e}_j$.

2. *Mechanical stiffness*: Mechanical stiffness is the object's ability to resist deformation. Note that large deformation will not cause the model to break, as long as the stress within the model is not beyond the yield stress (Chen et al.). Since too much deformation will affect the appearance of printed object, the deformation of the model should be controlled as

$$\|\mathbf{d}_i\| \leq d_{\max} \tag{8}$$

where $\mathbf{d}_i$ is the deformation displacement of node $\mathbf{v}_i$. The local deformation of the surface under loads shall be small (see Eqs. (3) and (4)), while the overall structure of designed model can have relatively large deformation.

3. *Radius bounds*: The radii constraint in Eq. (5) shall be fulfilled. For the beam structure, buckling will happen before the material reach its yield limit and greatly decrease the strength of whole structure if the beam is too slender. Therefore each strut must satisfy the following constraint to avoid the Euler buckling,

$$r_j \geq l_j/\alpha \tag{9}$$

where l_j is the length of strut $\mathbf{e}_j$ and α is the slenderness ratio which is set to be 60 in our experiments (also see Wang et al., 2013). Moreover, to make the supporting structure printable, each strut radius should be no less than the

Please cite this article in press as: Zhang, X., et al. Medial axis tree—an internal supporting structure for 3D printing. Comput. Aided Geom. Des. (2015), http://dx.doi.org/10.1016/j.cagd.2015.03.012

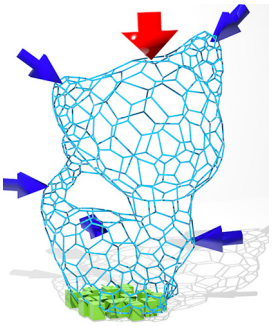

Fig. 10. Loads on a kitten model.

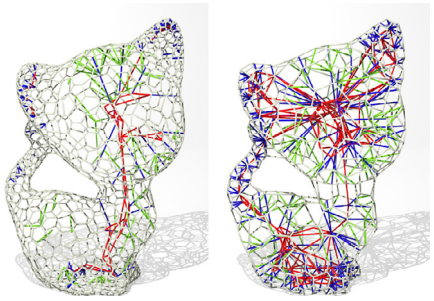

(a) 10 N (b) 100 N

Fig. 11. The results of topology optimization are influenced by applied loads.

minimum printing resolution of the 3D printer with which objects are fabricated. So the printability constraint is added for each strut as

$$r_j \geq \eta \tag{10}$$

where η is the minimum printing resolution.

5.2. Optimization

5.2.1. Load combination

The concept of "load combination" (Wen, 1990) from civil engineering is used to guide the assignment of loads for optimization. There are two steps in defining the load condition. First, the position and direction of loadings are recognized, with Stava's algorithm of assigning the location of loadings at the model's convex hull (Stava et al., 2012). Vertices near to each other of the convex hull are clustered, by a K-medoid algorithm and the load acts only on the cluster centers. The direction of the load on the cluster center is chosen as the average direction of the outer normal directions of the convex hull points. User can also specify additional loads for the model, for example user may add a vertical pinch force on the back of "horse" model.

Then in the second step, the magnitudes of the loads are determined by considering the probability of defined load conditions. According to engineering practice, the loads are classified into two kinds, which are the dead loads, corresponding to loads with largest probability, and the movable loads with lower probability.

The permanent loads, such as the gravity, are deemed as dead loads. Typical loads for the model, which corresponds to the working condition with largest possibility, such as the pinch force L^p_{kitten} on the head of "kitten" model, can also be deemed as dead loads, shown as the force in red in Fig. 10. Other load conditions are classified as movable loads, for example a pinch force on the tail of "kitten" model, shown as the force in blue on the tail. In our design, for models like kitten, sofa, horse and taurus, one kind of pinch load and the gravity are applied as dead loads. For bird model, which has typical symmetric shape, two pinch loads on the wings in separate directions and gravity are set as dead loads. Other loads recognized by the above algorithm are classified as movable loads.

The final load is set as the combination of defined loads $\mathbf{L}$ by Eq. (11), in which $\mathbf{L}_i^D$ represents the dead loads and $\mathbf{L}_j^M$ the movable loads. The magnitudes of $\mathbf{L}_i^D$ and $\mathbf{L}_j^M$ are chosen according to model's function. The coefficient p_j reflects the probability of the movable working condition, which is calculated by considering the proportion of area a_j on convex hull face corresponding to convex hull center point j (see Eq. (12)). The magnitudes of applied force will affect the optimization results, especially the results of topology optimization. An example is shown in Fig. 11, and the magnitudes of applied forces are set as $\|\mathbf{L}_i^D\| = \|\mathbf{L}_j^M\| = 10$ N and $\|\mathbf{L}_i^D\| = \|\mathbf{L}_j^M\| = 100$ N separately. With the aforementioned algorithm, the working condition can be determined.

$$\mathbf{L} = \sum \mathbf{L}_i^D + \sum \mathbf{L}_j^M p_j \tag{11}$$

$$p_j = \frac{a_j}{\sum a_j} \tag{12}$$

5.2.2. Partition method

A partition based structure optimization is proposed. A suitable number n which represents the number of design variables is prescribed. In practice, to assure the efficiency, n should not exceed 60. In our experience the optimization result is not sensitive to n, which is usually set as 30. Mechanical analysis is carried out on structure with same radii under the combined loads condition defined in previous section, then the bars in the structure are sorted according to their stress

Please cite this article in press as: Zhang, X., et al. Medial axis tree—an internal supporting structure for 3D printing. Comput. Aided Geom. Des. (2015), http://dx.doi.org/10.1016/j.cagd.2015.03.012

states and evenly divided into n groups. Bars in each group share the same radius, and all the radii are the variables of the optimization. The number of design variables in the structure is greatly reduced, compared with Wang's method to set all the radii of bars as design variables (Wang et al., 2013). In topology optimization, according to our algorithm, the inner bars and outer bars shall be put into different groups. Therefore a pre-partition is carried out to separate the inner bars and outer bars into two groups, and then further partition according to stress states is carried out within each group.

5.2.3. Optimization

Initialized by the medial axis trees structure designed by our algorithm, topological and volume optimization are carried out. In topological optimization, bars which contribute little to the structure's strength and stiffness are identified and deleted. Then the volume optimization is carried out to decide the radii of remaining bars in the medial axis tree to obtain model with least amount of material while meeting various constraints.

In both optimization, the objective function is expressed as the total volume of all struts in designed supporting structure, i.e.,

$$\mathrm{Vol}(\mathbf{r}) = \sum_{\mathbf{e}_j \in E} \pi r_j^2 l_j \tag{13}$$

where strut radii $\mathbf{r} = (r_1, \cdots, r_{|E|})$ are variables.

In topology optimization, the buckling constraint and printable constraint on the radii of bars are replaced by a looser one, as shown in Eq. (14), and the topology is updated after optimization calculation by removing bars with very small radii. In application, for models designed for uPrint Plus printer, we delete bars with radii less than the printer's precision η. To maintain the minimum completeness of medial axis tree structure, outer boundary struts are subject to a different constraint to avoid being removed.

$$r_{outer} \geq \eta, r_{inner} \geq 0 \tag{14}$$

The problem solved in topology optimization can be formulated as

$$\begin{array}{ll} \min_{\mathbf{r}} & \mathrm{Vol}(\mathbf{r}) \\ \text{s.t.} & \{(7), (8), (14)\} \end{array} \tag{15}$$

After the topology of the medial axis trees are determined, we can then carry out the following size optimization to modify the radii of the bars.

$$\begin{array}{ll} \min_{\mathbf{r}} & \mathrm{Vol}(\mathbf{r}) \\ \text{s.t.} & \{(7), (8), (5), (9), (10)\} \end{array} \tag{16}$$

To solve both optimization problems, we use the solver of mechanical analysis software Ansys®. The first order optimization method is used, in which the derivative information is calculated and used in optimization, which is described in Section 20.3 of Inc, 2009. Generally optimized results can be obtained in less than 15 circulations.

6. Experiment results

6.1. Results

We test our algorithm with several models and print them using FDM 3D printers, Stratasys® uPrint SE and uPrint SE Plus with build size 203 × 203 × 152 mm. The printing materials used are ABS and ABS Plus in white and the support material is SR-30 soluble (Stratasys, 2012). We also test our model with a Projet® 3500 HD*Max* printer using Multi Jet Modeling (MJM) technology, which has a much higher precision. In printing the model with complete outer surface, e.g. the kitten in Fig. 3(n), a hole is added on the model's bottom to facilitate the cleaning process. The parameters of the printer and the material properties are listed in Table 1. The printed models are shown in Fig. 12. The maximum length of bounding box of the printed models are 10 cm (except for the Taurus model with maximum size 5 cm).

We break down the time cost for processing and printing a model into 3 parts: initial supporting structure generation, optimization, and printing. The initial structure generation stage takes less than 2 minutes for most models. The optimization stage takes about 50 minutes to complete, and about another 20 minutes to produce a satisfactory result ready for printing, for an initial structure with 1101 nodes and 2672 struts. The first two stages are tested on a Windows PC with i7 CPU and 16G RAM. The printing stage with a uPrint SE printer takes about 5 hours for a model of 10 cm in height.

Fig. 13 shows the detailed data in model processing. The "horse" model is used to illustrate our process of optimization, as shown in Fig. 14. A whole list of results is shown in Table 3. The volume of surface is calculated by multiplying the area of surface by thickness which is set as 1 mm. The material parameters are set according to ABS material, whose $E = 1807$ MPa, $v = 0.35$ and constraints $\sigma_{\max} = 41$ MPa, $w_{\max} = 0.003$ m. The applied loads on Kitten, Horse and Taurus are set as $\|\mathbf{L}_i^D\| = \|\mathbf{L}_j^M\| = 10$ N, on Great wall as $\|\mathbf{L}_j^M\| = 10$ N, and the Bird model with loads $\|\mathbf{L}_i^D\| = 2$ N, and $\|\mathbf{L}_j^M\| = 0.5$ N.

Please cite this article in press as: Zhang, X., et al. Medial axis tree—an internal supporting structure for 3D printing. Comput. Aided Geom. Des. (2015), http://dx.doi.org/10.1016/j.cagd.2015.03.012

Table 1
The printers and printing material we used for printing.

Printer	uPrint SE	uPrint SE Plus	ProJet®
Technology	FDM	FDM	MJM
Precision (mm)	0.254	0.254	0.025
Material	ABS	ABS Plus	UV LCA
E (MPa)	1807	2265	–
σ_{max} (MPa)	41	36	49

Table 2
Experiment settings.

Speed	0.6 mm/minute
Pre-applied force	0.5 N
Stop condition	30% drop of force

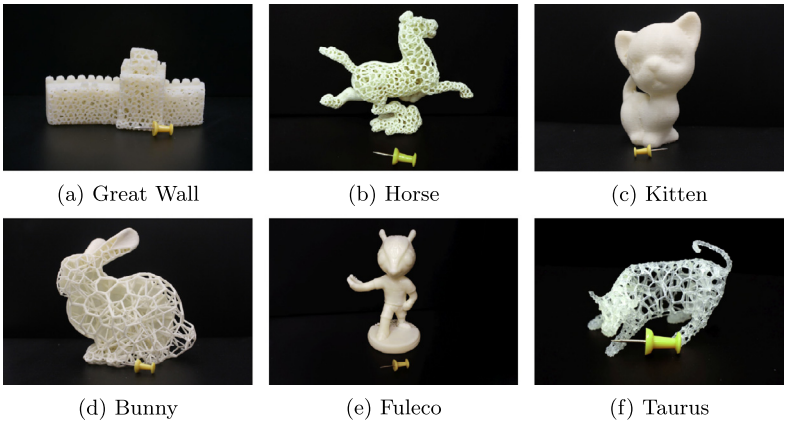

(a) Great Wall (b) Horse (c) Kitten

(d) Bunny (e) Fuleco (f) Taurus

Fig. 12. Printed objects. The models in (a), (c), (d) and (e) are printed by uPrint SE Plus printer; model (b) is printed by uPrint SE printer and (f) by Projet® 3500 HD*Max*.

Table 3
Optimization results for various models. The unit of volume is 1E-6 m^3, and stress as MPa. The thickness of surface is set as 1 mm. The volume of surface is calculated as multiplying the total area of surface by thickness.

Model	Solid vol.	Frame vol.	Surface vol.	Total vol.	Total ratio	Frame ratio
Kitten	127.19	9.39	17.17	26.56	20.88%	7.38%
Horse	28.19	4.80	9.29	14.09	50.0%	17.03%
Great wall	51.61	1.56	12.22	13.78	26.70%	3.02%
Bird	33.13	7.42	13.27	20.69	62.45%	22.40%
Taurus	89.68	13.75	16.37	30.12	33.59%	15.33%

6.2. Laboratory test

Standard compression test are carried out on printed models designed by our method, see Fig. 15. Two models, named as Fuleco and Sofa, are designed with our method with total volume 20.01 cm^3 and 20.37 cm^3. The obtained structure are covered with outer shells which are printed with thickness 1 mm. Only half of the model is cover by the shell to give us a better vision of the inner structure. Microcomputer control electronic universal testing machine with Model WDW-50C is used.

The settings of experiment are listed in Table 2. The force value against the displacement of the indenter is plotted, as shown in Fig. 16. When any strut in the model fails in the experiment, the detected value of force will drop, and if the value of force drops by more than 30%, we deem that the whole model is failed. Results showed that our designed Fuleco model can withstand force up to 140 N, when its neck was broken, satisfying the failing criterion. For the Sofa model, it can withstand more than 1400 N force, when the testing time ran out for a single test though the model itself didn't fail. The experiment results proved the strength of our designed model.

7. Comparisons

When comparing with different methods, we use the same criterion with the method under consideration. For each comparison, we use the same load configuration, material properties, constrains and model size for optimization, according to data provided by the original paper. Our method is judged to be better if our structure uses less material and withstands the same or larger loads. Different models are used when comparing with the different methods because there is no single common model used by all theses papers under comparison for which the needed information about the load configuration and resulting structure is provided.

Please cite this article in press as: Zhang, X., et al. Medial axis tree—an internal supporting structure for 3D printing. Comput. Aided Geom. Des. (2015), http://dx.doi.org/10.1016/j.cagd.2015.03.012

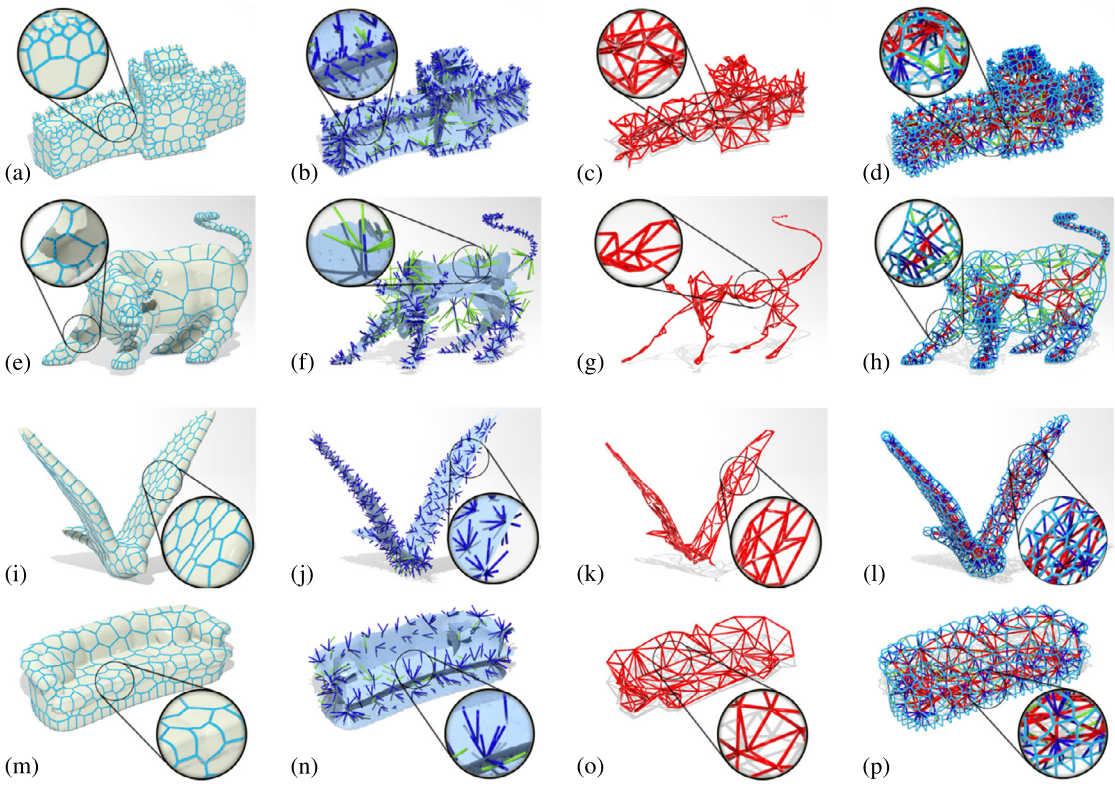

Fig. 13. Ours processing results for model Greatwall (a)–(d), Taurus (e)–(h), bird (i)–(l), and sofa (m)–(p). The first column is the input mesh and the hexagon mesh. The second column shows the medial axis tree trunks and branches. The third column is the medial axis tree roots and the last is a view of our whole structure respectively.

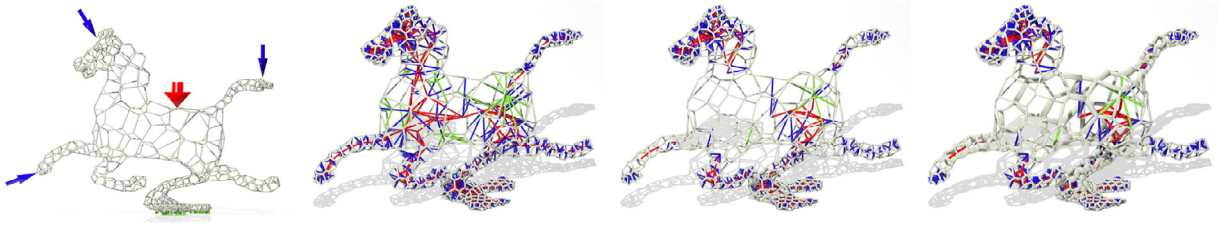

Fig. 14. Optimization process.

Note that we did not include in our comparison the outer supporting material added by FDM printers because the usage of outer supporting material usage is a printer-dependent issue. For example, powder-based printers do not need outer supporting material; moreover, even for FDM printers, different printer-specific settings result in different usages of the outer supporting material.

7.1. With Wang's frame structure (Wang et al., 2013)

We compare our modeling method with Weiming Wang's frame structure method. In both Wang's and our design, frame structure is adopted as the main component to resist load. The major difference is that Wang's model usually consist of a triangular surface frame structure plus few internal struts sensitive to the prescribed loads, but our model use a hexagon surface frame structure plus a symmetric tree like structure. For the Hanging Ball model, Wang et al. reported their model can resist 5 N with 2.875e4 mm^3 material for the frame. With our design, the material cost of the frame is 1.619e4 mm^3. With Wang's optimization method, all the inner structures of Hanging Ball are deleted, while with our method the MA Tree structure near the neck which connects the Ball and the base are remained, which greatly increase the strength of the model, and shows the effectiveness of our method (shown in Fig. 17(a) and (d)).

Please cite this article in press as: Zhang, X., et al. Medial axis tree—an internal supporting structure for 3D printing. Comput. Aided Geom. Des. (2015), http://dx.doi.org/10.1016/j.cagd.2015.03.012

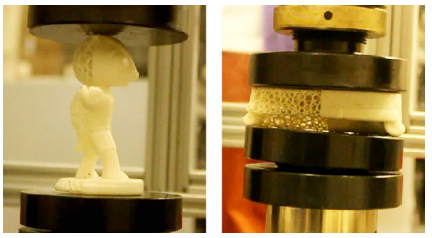

(a) Fuleco (b) Sofa

Fig. 15. The experiments.

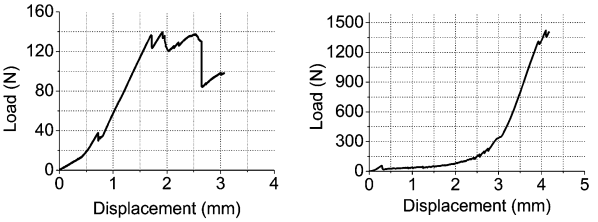

(a) Fuleco (b) Sofa

Fig. 16. Experiment results.

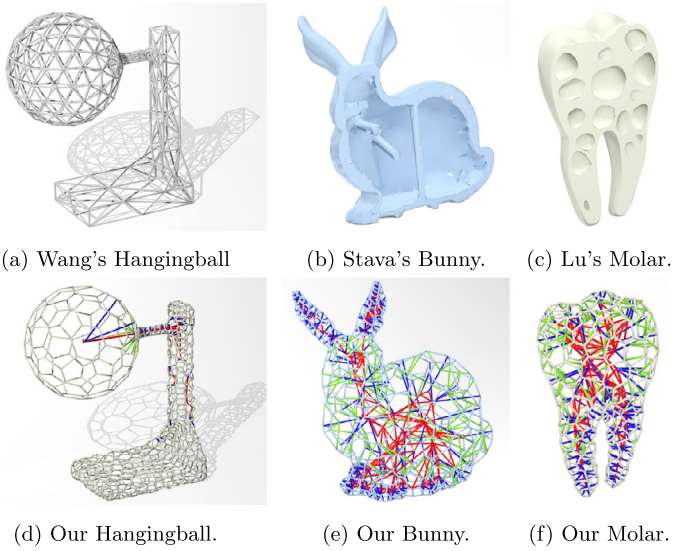

(a) Wang's Hangingball (b) Stava's Bunny. (c) Lu's Molar.

(d) Our Hangingball. (e) Our Bunny. (f) Our Molar.

Fig. 17. (a) (b) (c) shows the Hangingball, Bunny, and Molar model of Wang, Stava, and Lu respectively. (d) (e) (f) is our corresponding result.

7.2. With Stava's hollowing method (Stava et al., 2012)

We compare our modeling method with Stava's hollowing method in Fig. 17(b) and (e). With their method a hole is created in the Bunny model to save material and a few inner struts are added to maintain structural strength. The remaining problem with their method is that the thickness of the obtained hollowing model is difficult to choose, and the design scheme for the inner struts is not clear.

For the Bunny model, with Stava's method the designed model can resist 500 N with a mass of 84.3 g. Under same force setting for the bunny model, our medial axis tree structure needs 45.98 g, within which only 20.8 g (1.979e4 mm^3) material are used for the inner MA Tree structure.

7.3. With Lu's honeycomb-like interior structure (Lu et al., 2014)

The topology of honeycomb inspired both Lu's and ours design of supporting structure. We used hexagon frame structure for the surface, which has a high strength-to-weight ratio. We compare the Molar models designed by Lu's honeycomb-like interior structure method and our method. The root of the Molar model is fixed and external loads which sum to 600 N are applied on the top, which are same as Lu's settings. Their structure needs 9.64 cm^3 with maximum stress as 40.5 MPa (Lu et al., 2014) while our method needs 8.56 cm^3 with maximum stress as 34.1 MPa. The structures are shown in Fig. 17(c) and (f). Our MA Tree structure can produce structure with higher strength using less material compared with their honeycomb-like solid structure.

8. Conclusions

In this paper we introduced a *medial axis tree* structure to create a strong and light-weight model for 3D printing. Our designed structure consists of three components: (1) the medial structure which is near the medial axis of the input object and serves as the foundation of the whole supporting structure, (2) the hexagon boundary framework which is beneath the boundary surface and helps to disperse external loads and to resist shape deformation and (3) tree-like connecting bars

Please cite this article in press as: Zhang, X., et al. Medial axis tree—an internal supporting structure for 3D printing. Comput. Aided Geom. Des. (2015), http://dx.doi.org/10.1016/j.cagd.2015.03.012

serves as intermediate elements. These three components work together as an integrated supporting system. Topology and volume optimization are carried out to further improve the design. A number of experiment results show the capability of our method. Compared with other existing methods, our designed structure can withstand external loads from various directions, and produce stronger and lighter 3D printed objects.

Acknowledgements

We would like to thank the anonymous reviewers for their constructive comments. The work of Jiaye Wang and Changhe Tu is supported by the Natural Science Foundation of China (61332015, 61272242). The work of Zhouwang Yang is supported by the 973 Program 2011CB302400. The work of Wenping Wang is supported by the Research Grant Council of Hong Kong (718311E, 717813E). We sincerely thank Dr. Huang for his help in physical experiments.

References

Ali, M., Qamhiyah, A., Flugrad, D., Shakoor, M., 2008. Theoretical and finite element study of a compact energy absorber. Adv. Eng. Softw. 39 (2), 95–106.

Blum, H., et al., 1967. A transformation for extracting new descriptors of shape. Models for the Perception of Speech and Visual Form 19 (5), 362–380.

Bremicker, M., Chirehdast, M., Kikuchi, N., Papalambros, P., 1991. Integrated topology and shape optimization in structural design. J. Struct. Mech. 19 (4), 551–587.

Chandrupatla, T.R., Belegundu, A.D., Ramesh, T., Ray, C., 1991. Introduction to Finite Elements in Engineering. Prentice–Hall, Englewood Cliffs, NJ.

Chaussard, J., Couprie, M., Talbot, H., 2009. A discrete λ-medial axis. In: Proceedings of the 15th IAPR international conference on Discrete geometry for computer imagery. DGCI'09. Springer-Verlag, Berlin, Heidelberg, pp. 421–433. http://dl.acm.org/citation.cfm?id=1813270.1813312.

Chazal, F., Lieutier, A., 2005. The λ-medial axis. Graph. Models 67 (4), 304–331. http://dx.doi.org/10.1016/j.gmod.2005.01.002.

Chen, X., Zheng, C., Xu, W., Zhou, K. An asymptotic numerical method for inverse elastic shape design.

Culver, T., Keyser, J., Manocha, D., 1999. Accurate computation of the medial axis of a polyhedron. In: Proceedings of the Fifth ACM Symposium on Solid Modeling and Applications. SMA '99. ACM, New York, NY, USA, pp. 179–190.

Foskey, M., Lin, M.C., Manocha, D., 2003. Efficient computation of a simplified medial axis. In: Proceedings of the Eighth ACM Symposium on Solid Modeling and Applications. SM '03. ACM, New York, NY, USA, pp. 96–107.

Giesen, J., Miklos, B., Pauly, M., Wormser, C., 2009. The scale axis transform. In: Proceedings of the Twenty-fifth Annual Symposium on Computational Geometry. SCG '09. ACM, New York, NY, USA, pp. 106–115.

Hughes, T.J., 2012. The Finite Element Method: Linear Static and Dynamic Finite Element Analysis. Courier Dover Publications.

Inc, A., 2009. Theory reference for the mechanical APDL and mechanical applications.

Jiang, C., Wang, J., Wallner, J., Pottmann, H., 2014. Freeform Honeycomb Structures. Comput. Graph. Forum, vol. 33. Wiley Online Library, pp. 185–194.

Lu, Lin, Sharf, Andrei, Zhao, Haisen, Wei, Yuan, Fan, Qingnan, Chen, Xuelin, Savoye, Yann, Tu, Changhe, Cohen-Or, Daniel, Chen, Baoquan, 2014. ACM Trans. Graph. 33 (4) (Proc. SIGGRAPH).

Meshmixer, 2014. http://www.meshmixer.com/. accessed: 2014-11-28.

Miklos, B., Giesen, J., Pauly, M., 2010. Discrete scale axis representations for 3d geometry. In: ACM SIGGRAPH 2010 Papers. SIGGRAPH '10. ACM, New York, NY, USA, pp. 101:1–101:10.

Nieser, M., Palacios, J., Polthier, K., Zhang, E., 2012. Hexagonal global parameterization of arbitrary surfaces. IEEE Trans. Vis. Comput. Graph. 18 (6), 865–878. http://dx.doi.org/10.1109/TVCG.2011.118.

Park, H.-S., Jun, C.-H., 2008. A simple and fast algorithm for k-medoids clustering. Expert Syst. Appl. 36 (2), 3336–3341. http://dx.doi.org/10.1016/j.eswa.2008.01.039. http://linkinghub.elsevier.com/retrieve/pii/S095741740800081X.

Pietroni, N., Tonelli, D., Puppo, E., Froli, M., Scopigno, R., Cignoni, P., 2014. Voronoi grid-shell structures. arXiv:1408.6591.

Shapeways, 2012. Creating hollow objects. http://www.shapeways.com/tutorials/creating-hollow-objects.

Stava, O., Vanek, J., Benes, B., Carr, N., Měch, R., 2012. Stress relief: improving structural strength of 3d printable objects. ACM Trans. Graph. 31 (4), 48:1–48:11. http://dx.doi.org/10.1145/2185520.2185544.

Stratasys, 2012. uprint se plus specs. http://www.stratasys.com/3d-printers/idea-series/uprint-se-plus.

Timoshenko, S., Woinowsky-Krieger, S., Woinowsky-Krieger, S., 1959. Theory of Plates and Shells, vol. 2. McGraw–Hill, New York.

Tymrak, B.M., Kreiger, M., Pearce, J.M., 2014. Mechanical properties of components fabricated with open-source 3-d printers under realistic environmental conditions. Mater. Des. 58 (0), 242–246.

Wang, W., Wang, T.Y., Yang, Z., Liu, L., Tong, X., Tong, W., Deng, J., Chen, F., Liu, X., 2013. Cost-effective printing of 3d objects with skin-frame structures. ACM Trans. Graph. 32 (6), 177:1–177:10. http://dx.doi.org/10.1145/2508363.2508382.

Wen, Y.-K., 1990. Structural Load Modeling and Combination for Performance and Safety Evaluation, Developments in Civil Engineering. Elsevier Science Ltd.

Yan, D.-M., Lévy, B., Liu, Y., Sun, F., Wang, W., 2009. Isotropic remeshing with fast and exact computation of restricted Voronoi diagram. In: Proceedings of the Symposium on Geometry Processing. SGP '09. Eurographics Association, Aire-la-Ville, Switzerland, Switzerland, pp. 1445–1454. http://dl.acm.org/citation.cfm?id=1735603.1735629.

Please cite this article in press as: Zhang, X., et al. Medial axis tree—an internal supporting structure for 3D printing. Comput. Aided Geom. Des. (2015), http://dx.doi.org/10.1016/j.cagd.2015.03.012